Poroelasticity with Implication in Earth Sciences

Alex Cheng
University of Mississippi

Presented at
National Central University, Taiwan
January 5, 2018

Outline

- Porous materials
- Pioneers
- Poroelastic mechanisms
- Physical phenomena and applications

POROUS MATERIALS

(a) Sand

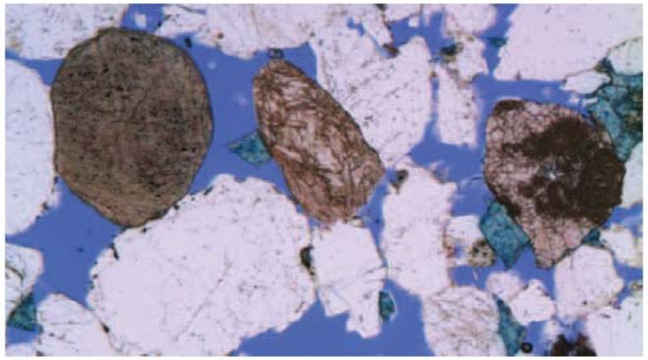

(b) Sandstone

(c) Volcanic rock

(d) Fractured rock

(e) Pervious concrete

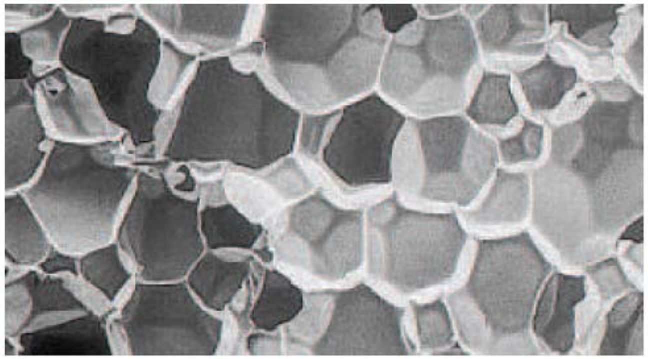

(f) Polyurethane foam

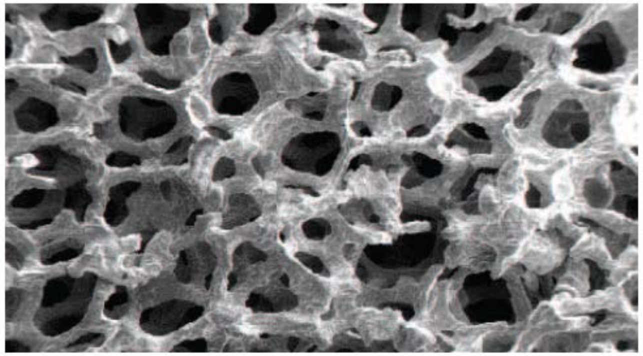

(g) Metal foam

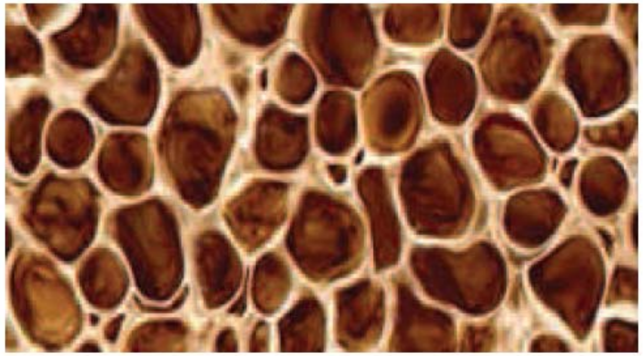

(h) Bone with osteoporosis

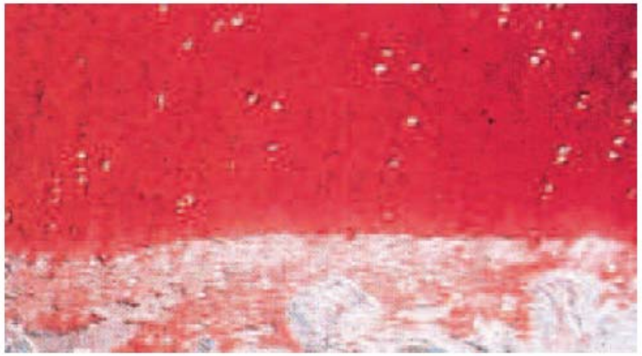

(i) Articular cartilage

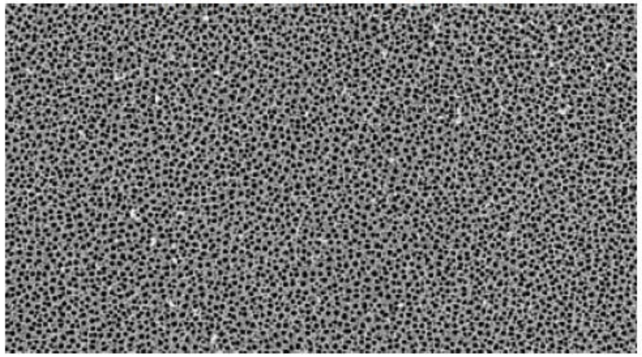

(j) Nanoporous alumina

PIONEERS

Leonardo da Vinci (1452-1519)

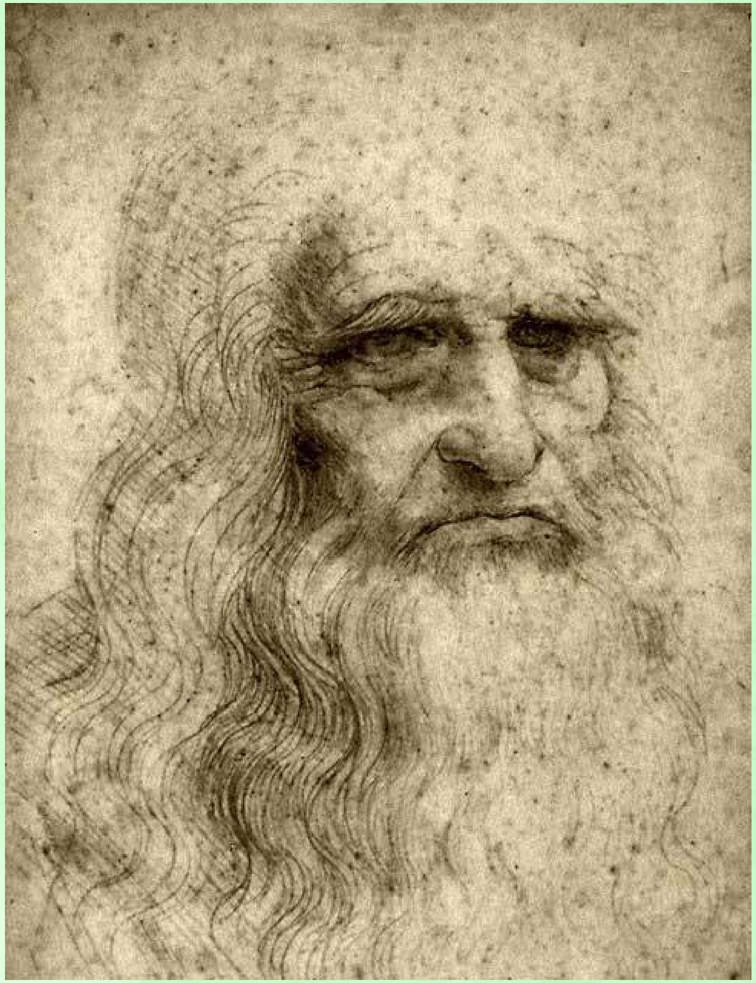

Codex Leicester (1506-1510)

The Earth is a living body. Its soul is its ability to grow. This soul, which also provides the Earth with its bodily warmth, is located in the inner fires of the Earth, which emerge at several places as baths, sulfur mines or volcanoes. Its flesh is the soil, its bones are the strata of rock, its cartilage is the tufa, its blood is the underground streams, the reservoir of blood around its heart is the ocean, the systole and diastole of the blood in the arteries and veins appear on the Earth as the rising and sinking of the oceans.

Karl von Terzaghi (1883-1963)
Father of Soil Mechanics

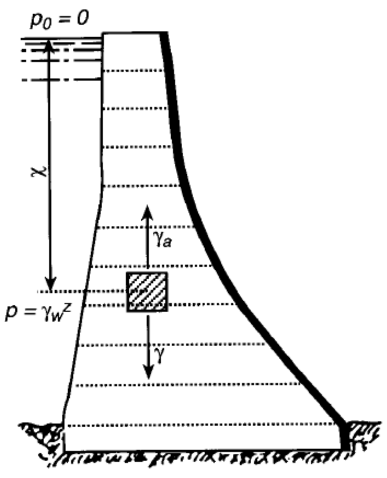

Fig. 3. Uplift in dams (Fillunger, 1913)

Controversy Between Terzaghi and Fillunger (Father of Mixture Theory)

Controversy on

- What is the role of pore pressure in the uplift, friction, and sliding failure of masonry dams?
- Does pore pressure change the ultimate strength of concrete?
- The consolidation phenomenon: what is the role of pore pressure on the volumetric deformation of porous materials?
- Resulting to the suicide of Fillunger

Effective Stress

- Terzaghi: Intuitive approach based on experimental observation (1923).
- Fillunger: Theoretical derivation which is the forerunner of the present day mixture theory.
- Biot introduced the Biot effective stress in 1941.

Equation for effective stress

- Terzaghi: $P' = P - p$
- Fillunger: $P' = P - \varphi p$
- Biot: $P' = P - \alpha p$

Nur and Byerlee 1971 Experiment

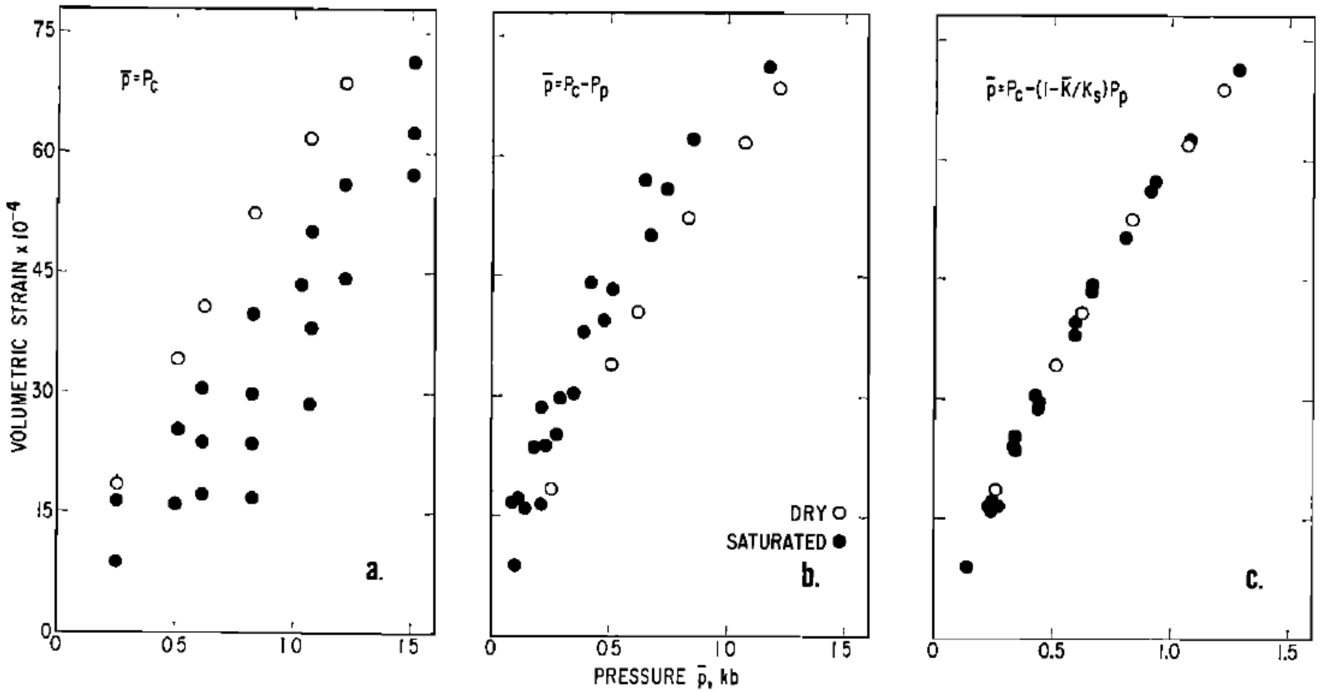

Fig. 2. Volumetric strain versus effective stress in porous Weber sandstone. (*a*) Strain versus confining pressure. (*b*) Strain versus the difference between confining and pore pressures. (*c*) Strain versus theoretical effective pressure. The open circles show the strain versus confining pressure in a dry confined sample.

Maurice A. Biot (1905-1985)
(Father of Poroelasticity)

"*We propose to show that a* ***linear theory of consolidation can be established by combining the theory of elasticity with Darcy's law of flow of a fluid through a porous material****. …* ***The element is assumed to be large compared to the pore size***." (Maurice Biot, 1935)

LE PROBLÈME DE LA CONSOLIDATION DES MATIÈRES ARGILEUSES SOUS UNE CHARGE

Note de M. M. Biot.

Nous nous proposons de montrer qu'une théorie linéaire de la consolidation peut s'établir en combinant la théorie de l'Élasticité avec la loi de Darcy d'écoulement d'un fluide à travers un matériau poreux.

Supposons que le squelette poreux considéré comme un milieu continu et homogène satisfasse aux hypothèses habituelles de la théorie de l'Élasticité. Faisons abstraction pour l'instant du liquide qui le remplit. Les tensions qui agissent sur un élément cubique de côté unité de ce milieu poreux sont de même nature que celles que l'on définit en Élasticité habituelle. L'élément est supposé grand par rapport à la dimension des pores. Ces tensions peuvent être désignées par les composantes,

$$\begin{matrix} \sigma_x & \tau_z & \tau_y \\ \tau_z & \sigma_y & \tau_x \\ \tau_y & \tau_x & \sigma_z \end{matrix}$$

Portons maintenant notre attention sur le liquide qui remplit les pores. Si ce liquide est à la pression q, il existe entre les faces de l'élément cubique considéré une tension normale isotrope,

$$\sigma = -(1-\alpha)\,q$$

où α est le pourcentage de la surface du cube occupé par le matériau solide du squelette.

Le système des forces qui agissent sur les faces de l'élément cubique considéré lorsque le matériau poreux est rempli de liquide à la pression q, est la somme des deux systèmes de tensions considérés ci-dessus et peut se représenter par les composantes

$$\begin{matrix} \sigma_x+\sigma & \tau_z & \tau_y \\ \tau_z & \sigma_y+\sigma & \tau_x \\ \tau_y & \tau_x & \sigma_z+\sigma\,. \end{matrix}$$

Ce système de forces intérieures doit être en équilibre, de sorte qu'on a ;

$$\begin{aligned} &\frac{\partial}{\partial x}(\sigma_x+\sigma)+\frac{\partial \tau_z}{\partial y}+\frac{\partial \tau_y}{\partial z}=0 \\ &\frac{\partial \tau_z}{\partial x}+\frac{\partial}{\partial y}(\sigma_y+\sigma)+\frac{\partial \tau_x}{\partial z}=0 \qquad (1) \\ &\frac{\partial \tau_y}{\partial x}+\frac{\partial \tau_x}{\partial y}+\frac{\partial}{\partial z}(\sigma_z+\sigma)=0 \end{aligned}$$

POROELASTIC MECHANISMS

Drained and Undrained Responses

$$\frac{\Delta V}{V} = -\frac{\Delta P}{K_u}$$

$$\frac{\Delta V}{V} = -\frac{\Delta P}{K}$$

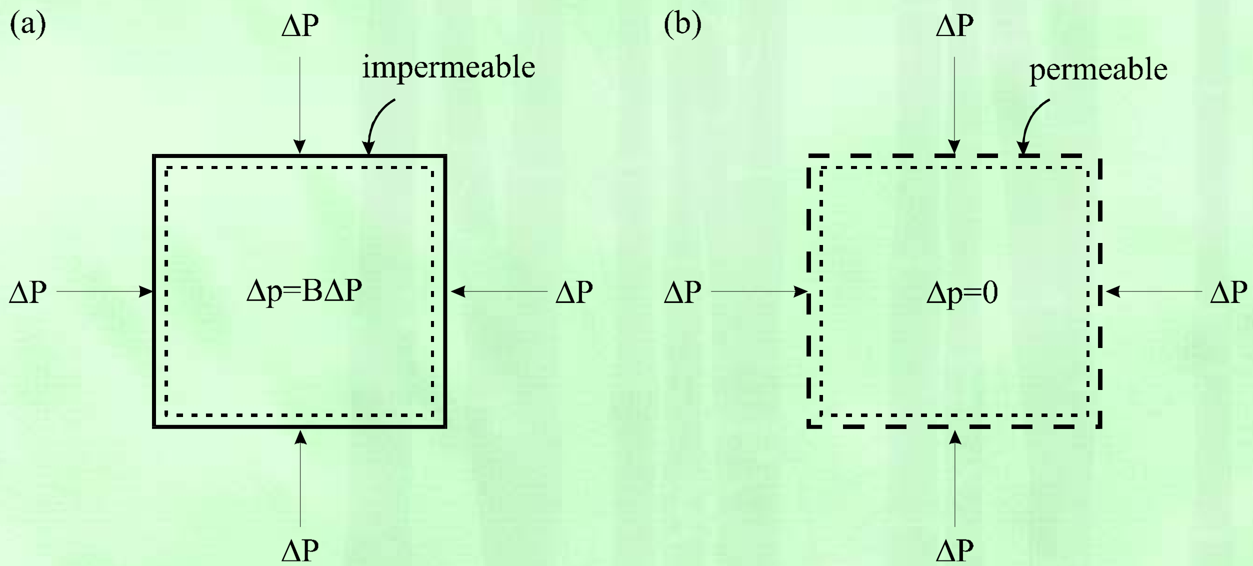

undrained

drained

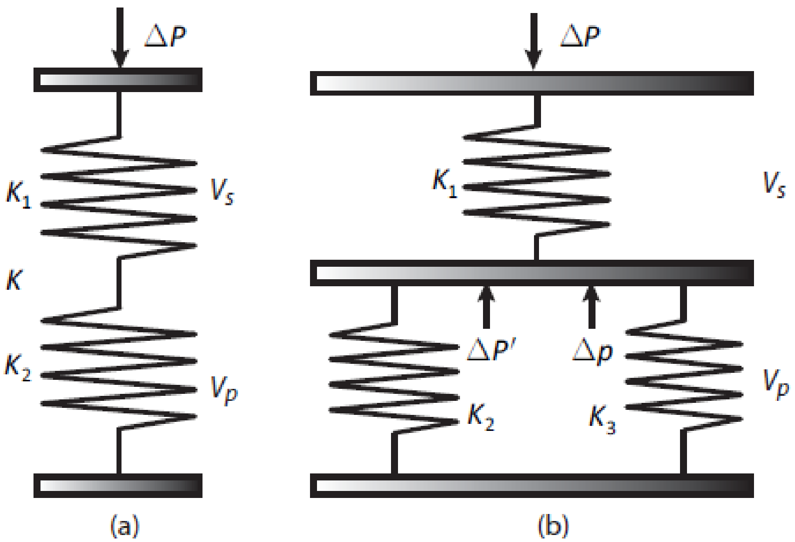

Figure 1.2 Spring analogy: (a) Series springs for drained bulk modulus, and (b) Parallel springs for undrained bulk modulus.

Skempton Pore Pressure Effect

$$B = \frac{\Delta p}{\Delta P}$$

$$B = \frac{K_f}{\phi K + K_f}$$

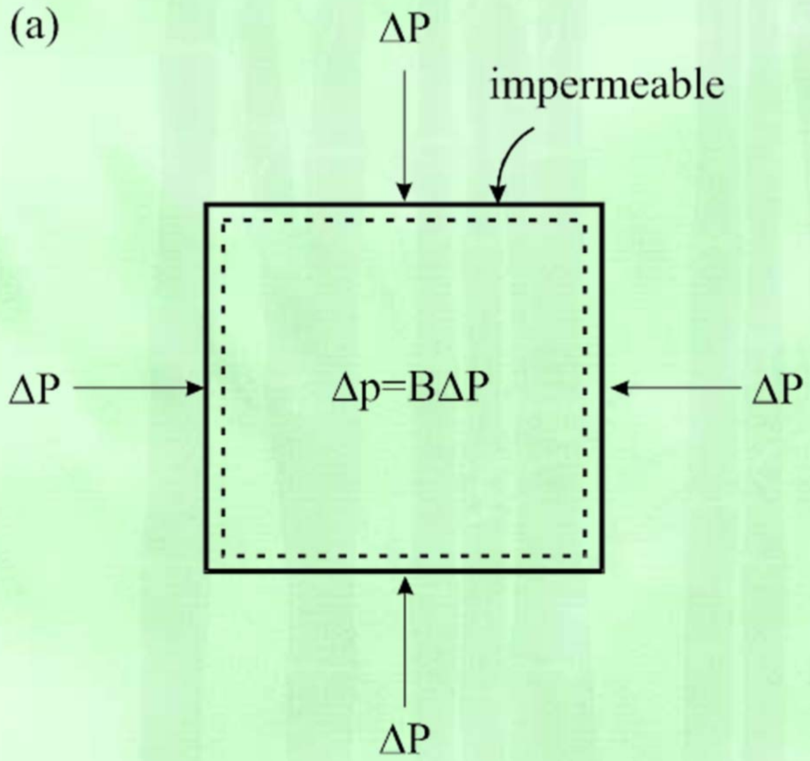

Effective Stress

Based on extensive historical study, de Boer called the attention to a controversy between Karl von Terzaghi (father of soil mechanics) and Fillunger (father of mixture theory) on the correct form of the effective stress. According to de Boer, the controversy is still not settled.

Equation for effective stress

- $P' = P - (? \times p)$
- Terzaghi: $P' = P - p$
- Fillunger: $P' = P - \varphi p$
- Biot: $P' = P - \alpha p$
- de Boer: $P' = P - (\alpha + \varphi - \alpha\varphi)\, p$
- Effective stress for volumetric deformation
- Effective stress for material failure

Biot Effective Stress

$$\frac{\Delta V}{V} = -\frac{1}{K}(\Delta P - \alpha \Delta p) \tag{1.22}$$

in which the left hand side is the volumetric strain of the frame, K is the (drained) bulk modulus of the frame, and α is the coefficient in question. The coefficient α defines the weighted contribution of pore pressure to the load reduction, and is called the effective stress coefficient. It has the value between 0 and 1.

$$\alpha = 1 - \frac{K}{K_s}$$

Porous Medium	α	β	η	K_p (N/m^2)	ν	ν_u	K_u (N/m^2)	B	M (N/m^2)	c (m^2/s)
Ruhr sandstone(1)	0.637	0.989	0.275	4.10×10^{8}	0.120	0.299	2.87×10^{10}	0.854	3.84×10^{10}	5.10×10^{-3}
Tennessee marble(1)	0.200	0.920	0.067	4.00×10^{9}	0.250	0.266	4.32×10^{10}	0.371	8.01×10^{10}	7.67×10^{-6}
Charcoal granite(1)	0.242	0.937	0.076	2.85×10^{9}	0.270	0.292	3.87×10^{10}	0.454	7.26×10^{10}	6.77×10^{-6}
Berea sandstone(1)	0.778	0.946	0.292	1.95×10^{9}	0.200	0.313	1.40×10^{10}	0.551	9.92×10^{9}	1.37×10^{0}
Westerly granite(2)	0.449	0.988	0.150	5.56×10^{8}	0.250	0.331	3.93×10^{10}	0.810	7.08×10^{10}	2.15×10^{-5}
Weber sandstone(3)	0.629	0.965	0.259	1.27×10^{9}	0.150	0.272	2.27×10^{10}	0.653	2.35×10^{10}	1.79×10^{-2}
Ohio sandstone(4)	0.729	0.929	0.284	2.20×10^{9}	0.181	0.280	1.32×10^{10}	0.498	9.01×10^{9}	3.96×10^{-2}
Pecos sandstone(4)	0.830	0.960	0.336	1.56×10^{9}	0.159	0.309	1.33×10^{10}	0.605	9.71×10^{9}	5.31×10^{-3}
Boise sandstone(5)	0.853	0.955	0.351	1.40×10^{9}	0.150	0.279	8.11×10^{9}	0.507	4.82×10^{9}	1.76×10^{0}
Gulf Mexico shale(6)	0.968	0.990	0.348	3.41×10^{8}	0.219	0.449	7.22×10^{9}	0.876	6.54×10^{9}	1.68×10^{-7}
Danian chalk(7)	0.725	0.913	0.256	1.05×10^{9}	0.227	0.357	6.96×10^{9}	0.726	6.97×10^{9}	4.39×10^{-5}
Hard sediment(8)	0.999	0.999	0.333	2.05×10^{7}	0.250	0.497	4.51×10^{9}	0.992	4.47×10^{9}	7.72×10^{0}
Soft sediment(8)	0.999	0.999	0.333	2.81×10^{7}	0.250	0.496	2.93×10^{9}	0.988	2.90×10^{9}	6.50×10^{-1}
Abyssal red clay(9)	1.000	1.000	0.004	1.42×10^{7}	0.498	0.500	2.79×10^{9}	0.993	2.77×10^{9}	3.99×10^{-6}
Rock salt(10)	0.119	0.993	0.040	1.74×10^{8}	0.250	0.274	2.33×10^{10}	0.926	1.81×10^{11}	1.69×10^{-7}
Coarse sand(11)	0.960	0.980	0.289	9.71×10^{7}	0.284	0.463	1.29×10^{9}	0.885	1.19×10^{9}	1.10×10^{-1}
Polyurethane foam(11)	0.940	0.941	0.237	8.05×10^{3}	0.331	0.500	8.93×10^{6}	1.06	1.01×10^{7}	2.76×10^{-4}
Wool felt(11)	0.910	0.931	0.260	8.82×10^{5}	0.299	0.493	3.63×10^{7}	1.06	4.25×10^{7}	1.63×10^{-5}
Cortical bone(12)	0.137	0.684	0.037	4.39×10^{9}	0.317	0.326	1.27×10^{10}	0.386	3.57×10^{10}	5.07×10^{-7}
Alundum(13)	0.602	0.791	0.234	1.65×10^{10}	0.182	0.200	3.37×10^{10}	0.113	6.31×10^{9}	1.65×10^{-1}

(1) Ref. [260, 575] (2) [260, 524, 575, 739] (3) [260, 524, 575] (4) [260, 722, 723] (5) [260, 287] (6) [6, 490] (7) [6, 278] (8) [36, 636]
(9) [367, 478] (10) [478, 552] (11) [420] (12) [206] (13) [722]

Table 3.2 Poroelastic constants for various materials—Derived constants.

Effective Stress for Failure (Pore Collapse)

- Experimental observations on sandstones, limestone, and granite showed that the ultimate strength and ductility of rocks are unique functions of the Terzaghi effective compressive stress.
- The first stage of compressive failure is likely to be characterized by the collapse of pore space than the yielding of solid phase.
- Porosity variation is a function of the Terzaghi effective stress only.

Extension of effective stress concept

- $P' = P - (? \times p)$
  - What if $(? \times p) > P$ such that $P < 0$ (tension)?
  - What if $p < 0$ such that $P' > P$ (more compressive)?

Pinch-off test

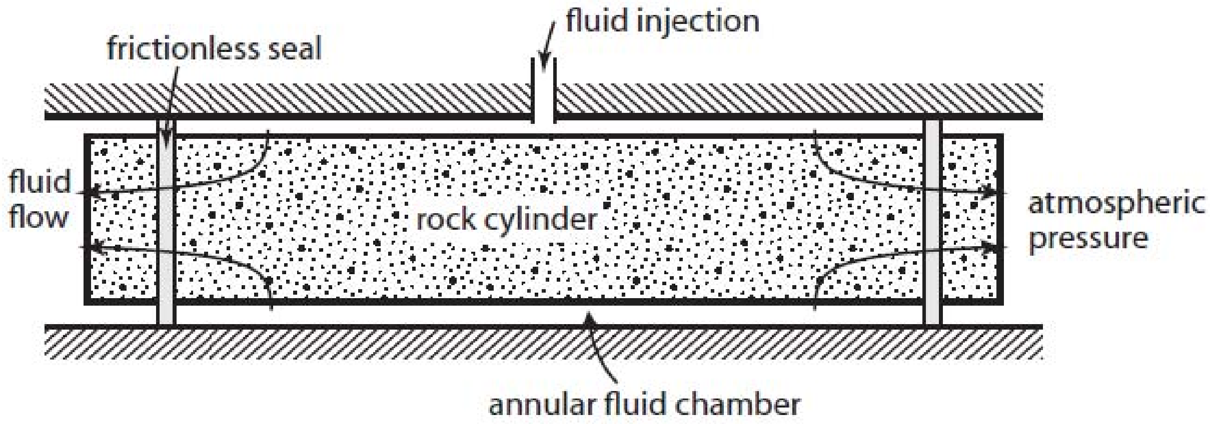

Figure 1.9 Pinch-off test to break a rock cylinder by tension.

Bridgman, P. W. (1912), Breaking tests under Hydrostatic pressure and conditions of rupture, *Philosophical Magazine*, **24**(139), 63-80.

How to build a sand castle?

- Which is more stable, dry sand, wet (partially saturated) sand, and fully saturated sand?
- Dry sand ($p = 0$), partially saturated sand ($p < 0$), fully saturated sand ($p > 0$)

Coal Cavitation

Mined cavitation burn pit

Coal Mine Outburst

POROELASTIC PHENOMENA

Mandel and Cryer Effect

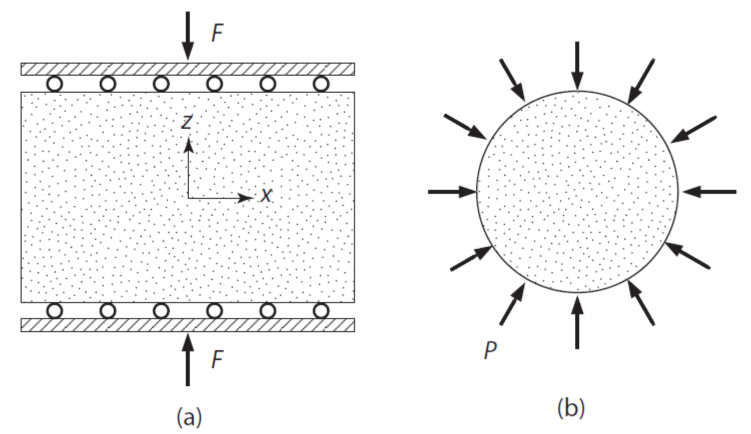

Figure 1.4 (a) Mandel problem, and (b) Cryer problem.

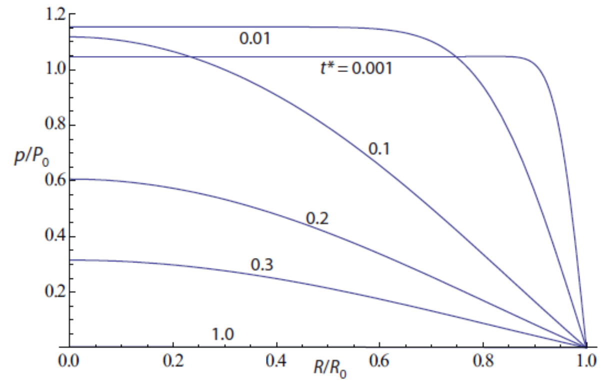

Figure 7.17 Normalized pressure distribution for the Cryer problem at various times, for an incompressible constituents model with $\nu = 0.25$.

Noordbergum & Rhade Effect

- Noordbergum effect: With the injection of fluid into the formation, the pressure head in a nearby observation well falls before it rises.

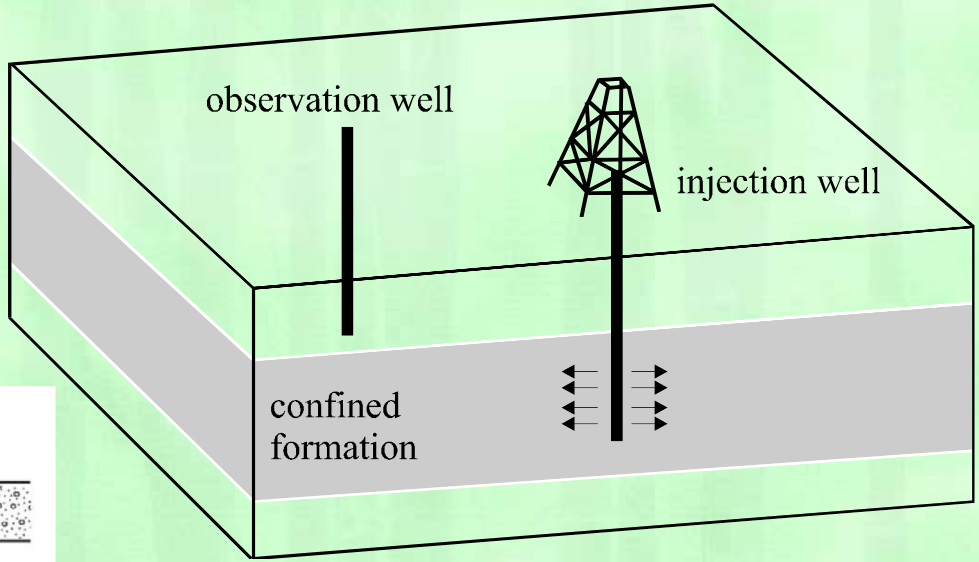

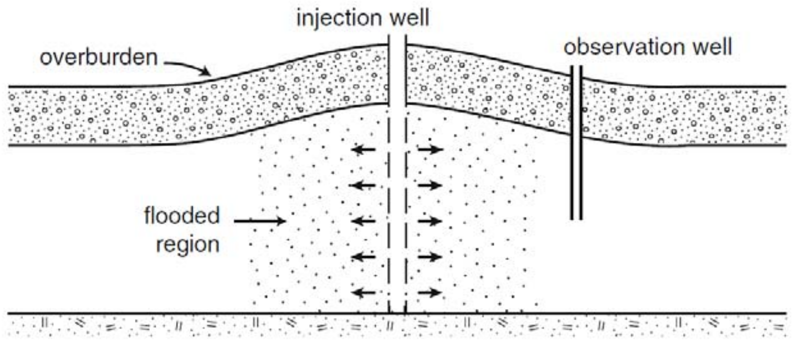

Fig. 1.5 Noordbergum-like effect due to uplift of overlain formation

Subsidence

Groundwater & Land Subsidence in California
In an average year, groundwater provides about 40% of California's water supply.
In the current drought, groundwater may account for 65% or more of the state's groundwater supply.
Subsidence in Santa Clara Valley has required various infrastructure construction & repairs, totaling more than $756 million
1925
1955
SAN JOAQUIN VALLEY
CALIFORNIA
BM S661
SUBSIDENCE 9M
1925-1977
1977
Subsidence from groundwater pumping in the San Joaquin Valley has been called the greatest human alteration of the Earth's surface.
Today, land subsidence is occurring at almost 1 ft/yr
By 1970, subsidence of more than 1 foot had affected more than half of the San Joaquin Valley — in some areas as much as 28 feet
Sustainable Conservation
http://www.suscon.org
Facts from http://californiawaterfoundation.org/uploads/1398291778-Subsidencesummaryreport-FINAL.pdf

Borehole Failure

- Compressive failure
- Mohr-Coulomb failure
- Tensile failure
- Mud weight design

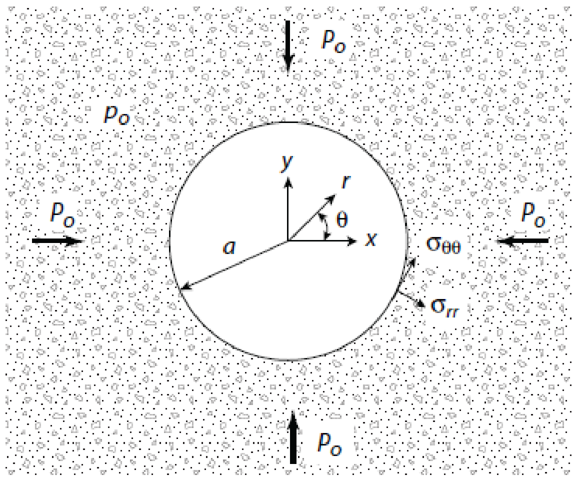

Figure 1.3 Borehole in an uniform stress field.

Borehole Drilling Design Software: Pbore-3D

Polar Charts

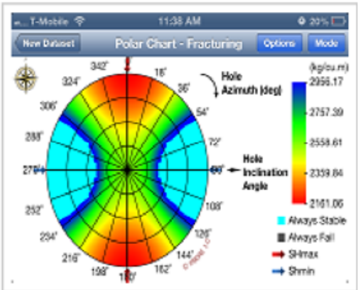

Mud window

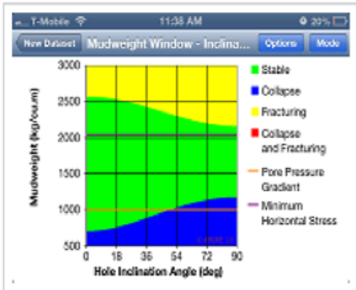

2D Plot

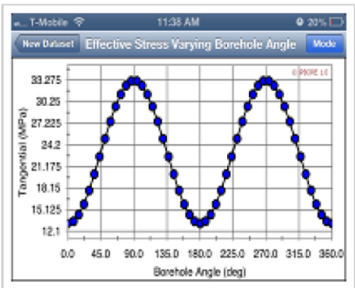

Failure region

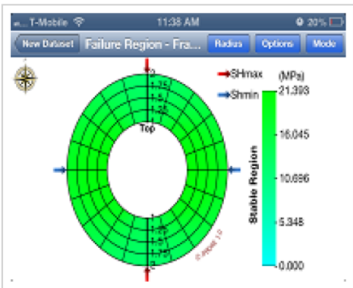

Polar Charts

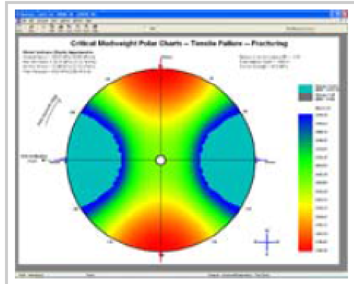

Mud window

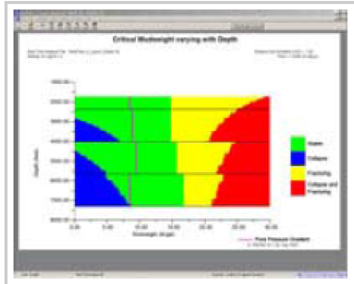

Contour Maps

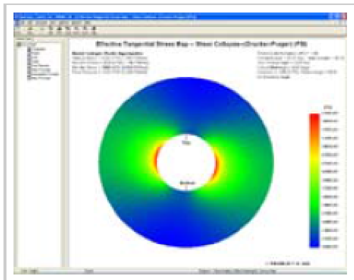

Fractures Rock Analyses

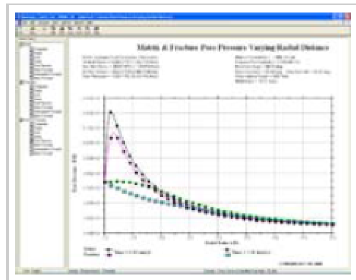

Slope Stability and Fault Slippage

(a)

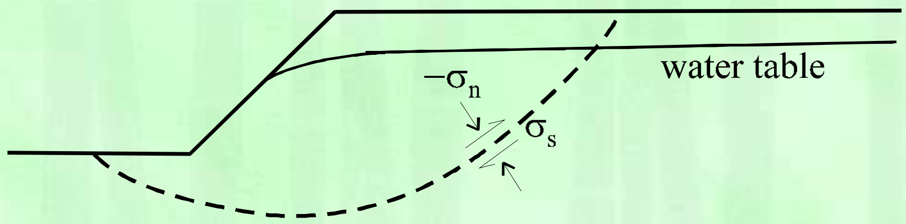

(b)

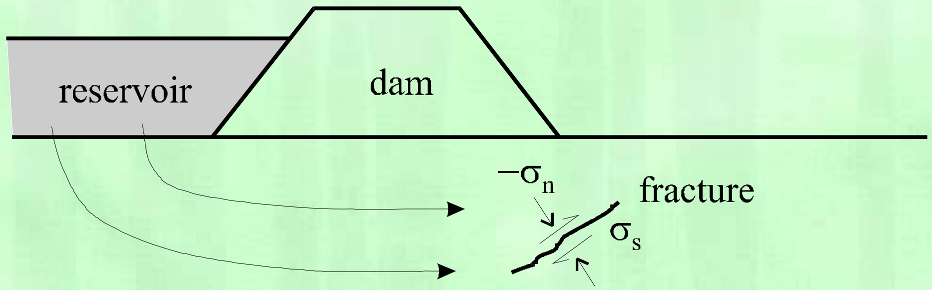

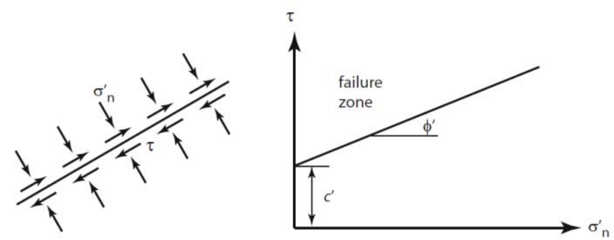

Fig. 1.6 Mohr-Coulomb shear failure criterion

Overthrust Faulting

Hubbert, M. K., and W. W. Rubey (1959), Role of fluid pressure in mechanics of overthrust faulting. 1. Mechanics of fluid-filled porous solids and its application to overthrust faulting, *Geological Society of America Bulletin*, 70(2), 115-166.

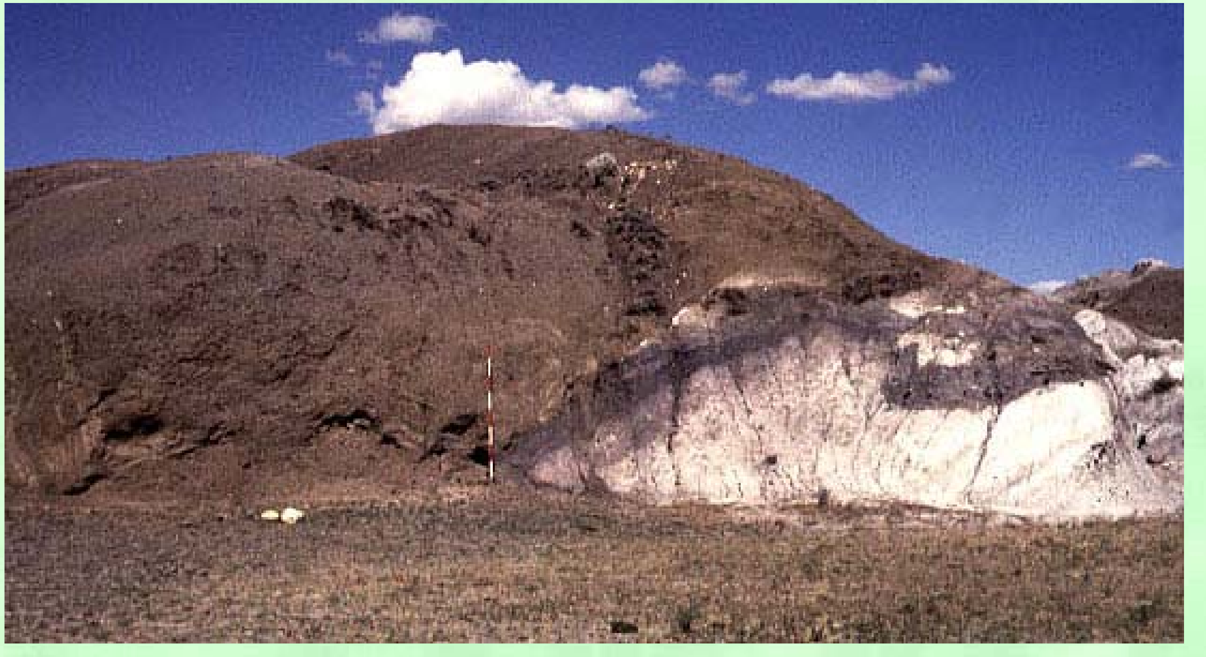

Overthrust of brown Eastend Formation (left) onto white/gray Whitemud Formation (right), Dirt Hills, Saskatchewan, Canada.

Beer Can Experiment

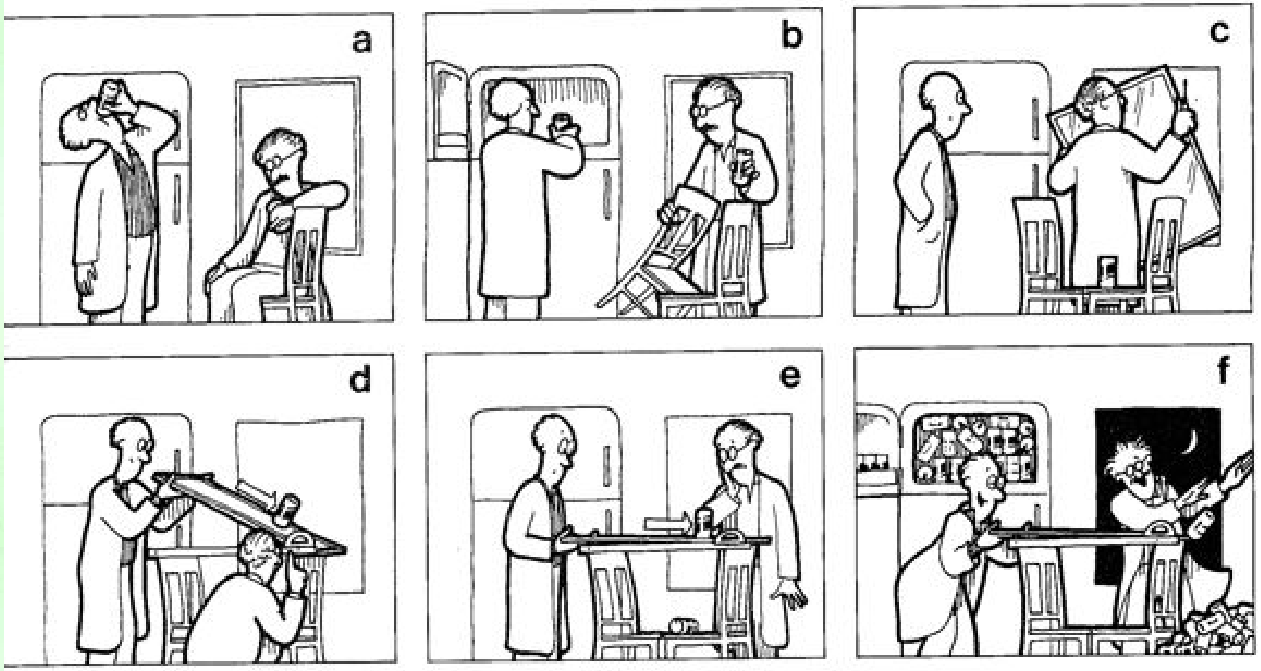

Figure 6.107 The famous beer can experiment. (Artwork by D. A. Fischer.)

Liquefaction

- Acceleration and propagation of dilatational induced weight reduction causing particles to lose contact.
- Compression caused pore pressure reduces effective stress
- Cyclic loading caused soil compaction results in cyclic pore pressure built up.

Earthquake: Pore Pressure Observation

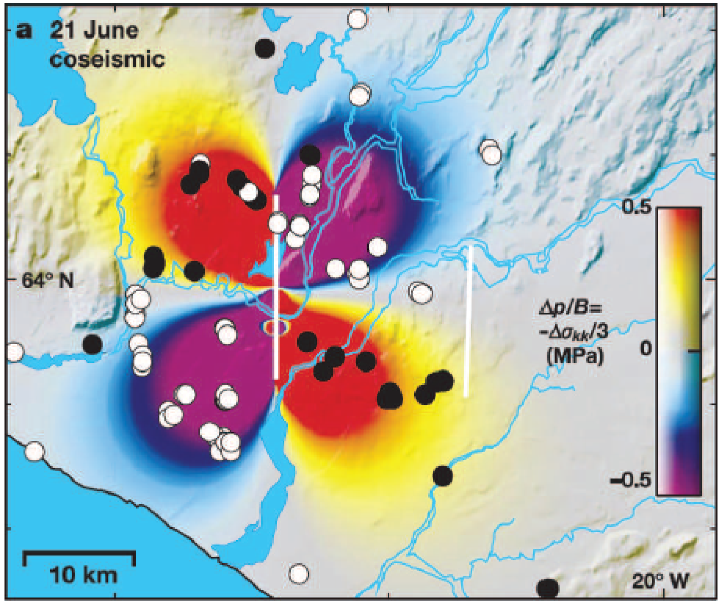

Figure 1.7 Coseismic water level changes in geothermal wells in South Iceland. Water level increase is shown in black dots and decrease in white dots. (From Jónsson *et al*. [405], with permission.)

Nature, 2003

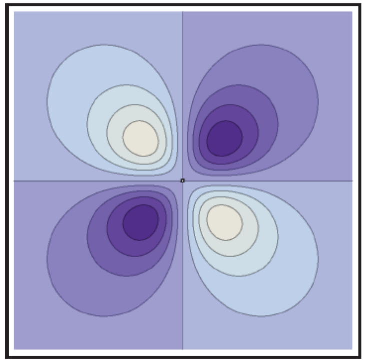

Figure 1.8 Contour plot of pore pressure generated by a slipping displacement discontinuity.

Earthquake Aftershock

Aftershocks Caused by Pore Fluid Flow?

Abstract. *Large shallow earthquakes can induce changes in the fluid pore pressure that are comparable to stress drops on faults. The subsequent redistribution of pore pressure as a result of fluid flow slowly decreases the strength of rock and may result in delayed fracture. The agreement between computed rates of decay and observed rates of aftershock activity suggests that this is an attractive mechanism for aftershocks.*

Nur, A., and J. R. Booker (1972), Aftershocks caused by pore fluid flow?, *Science*, *175*(4024), 885-887.

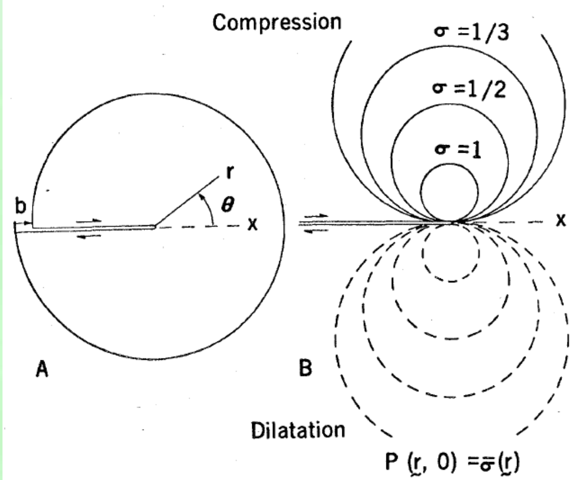

Fig. 1. (A) Representation of a fault's end by an edge dislocation with offset b; (B) the induced hydrostatic stress $\sigma(\mathbf{r})$. The initial pore pressure $P(\mathbf{r},0)$ is equal to $\sigma(\mathbf{r})$.

Fracking Induced Earthquake

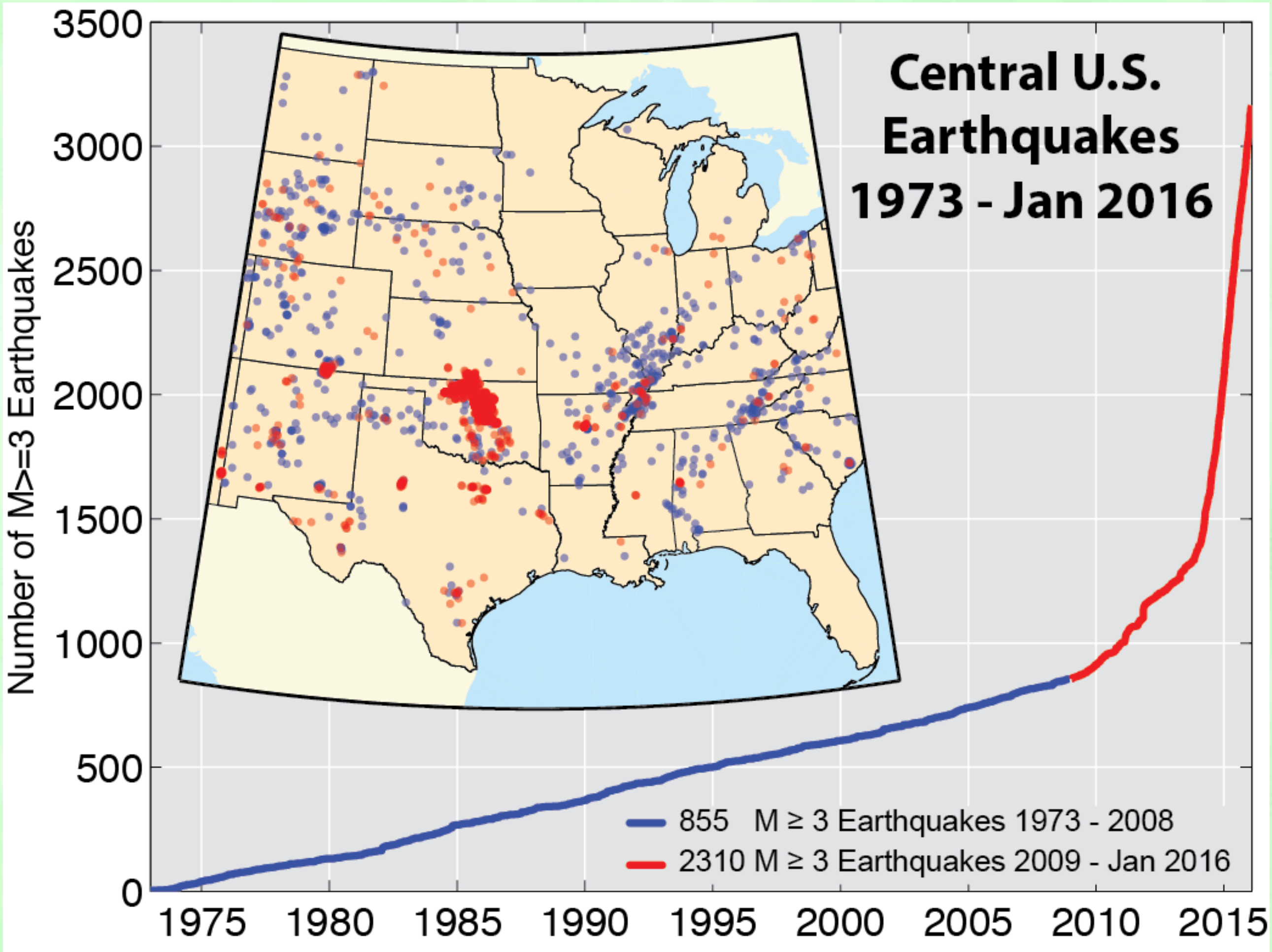

Water Wave and Seabed Interaction

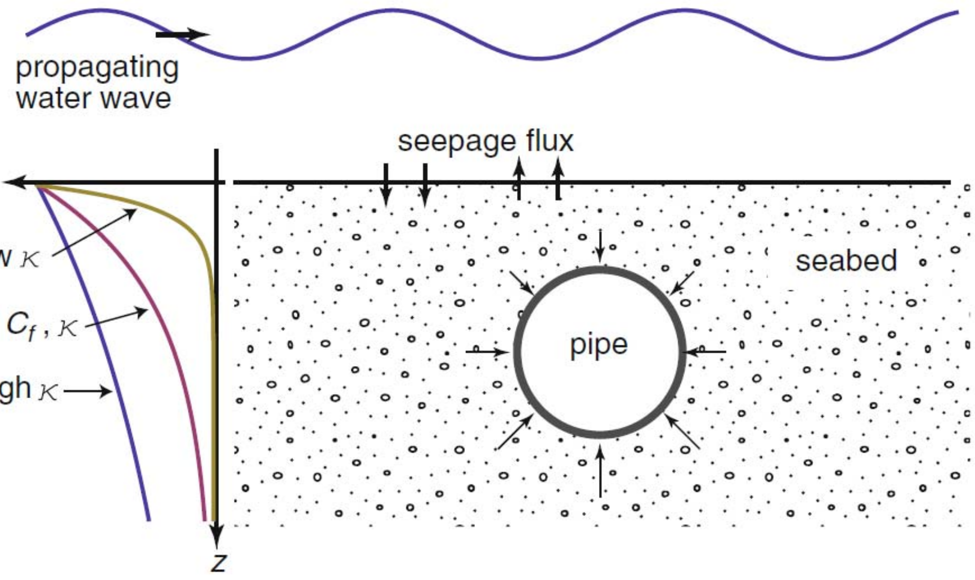

Fig. 1.11 Uplift force on a pipeline buried in sea bed

Formation Response to Tidal and Barometric Waves

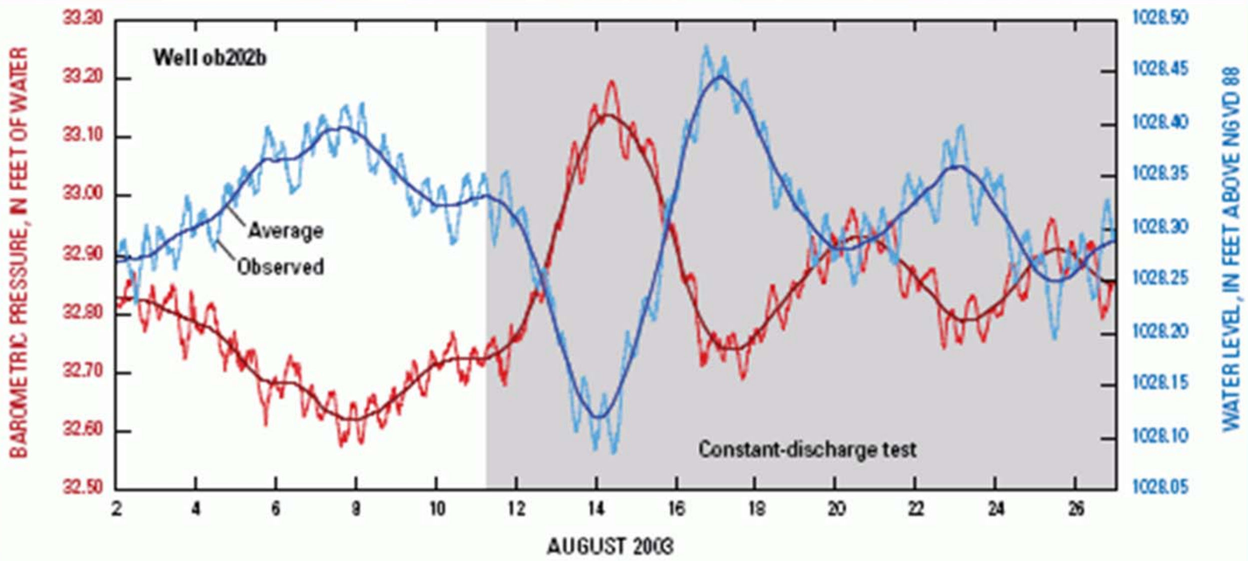

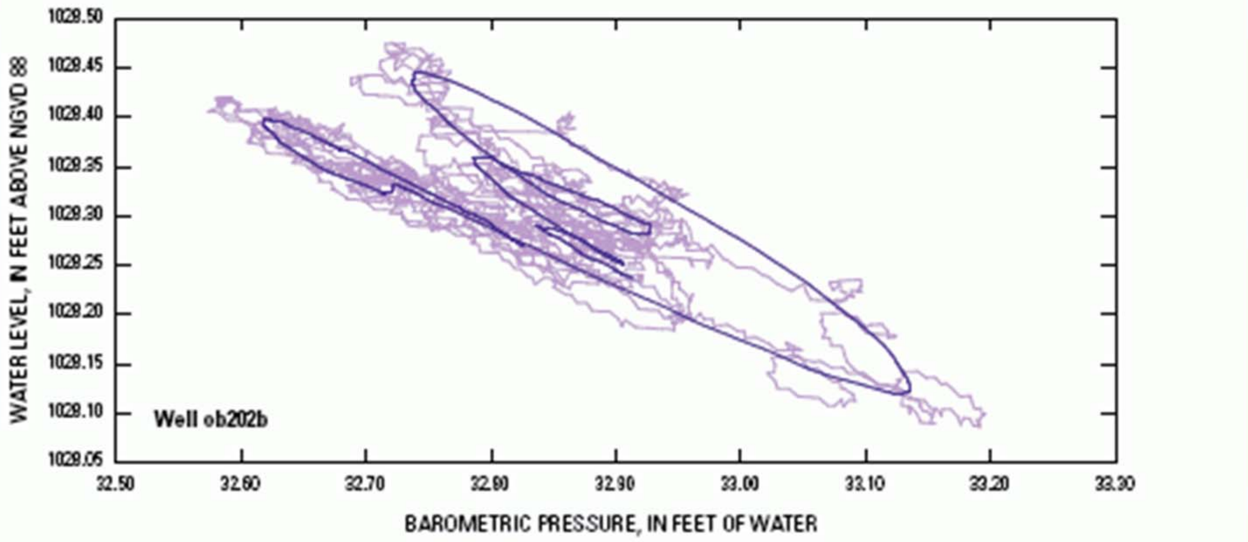

Poroviscoelasticity and Anelastic Strain Recovery

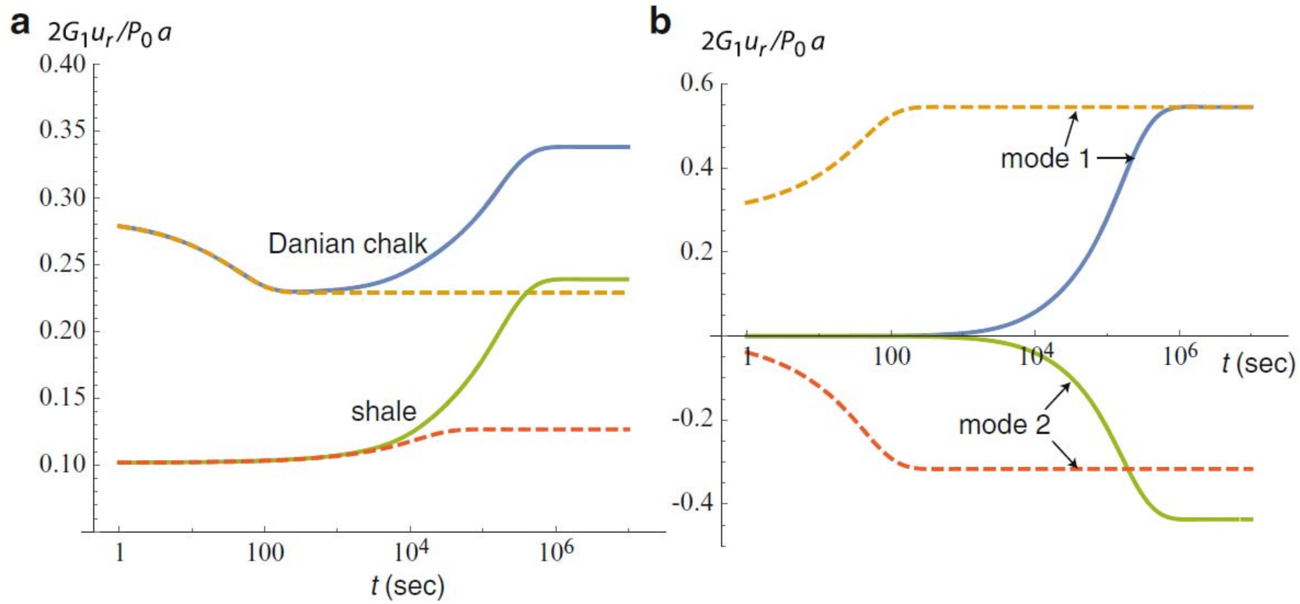

Fig. 10.9 (**a**) Radial displacement of retrieved cylindrical core, $u_r(r_o, t)$. *Solid line*: poroviscoelastic solution; *dashed line*: poroelastic solution. (**b**) The Danian chalk solution decomposed into mode 1 and mode 2 contributions. *Solid line*: viscoelastic contribution; *dashed line*: poroelastic contribution

Porothermoelasticity and Burst of Saturated Concrete in Fire

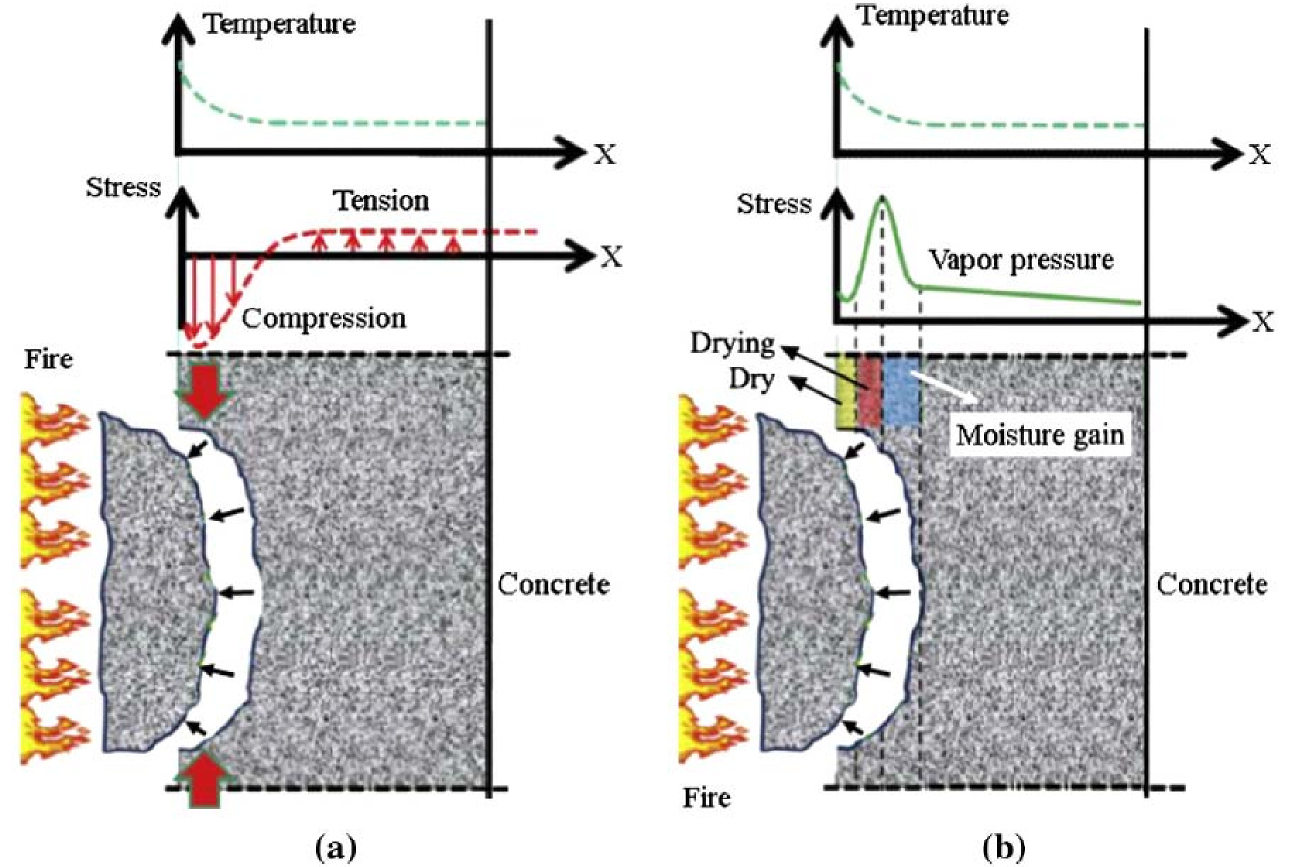

Fig. 1. Mechanisms of concrete spalling (**a**) Thermal stress theory; (**b**) Pore pressure theory [9].

Poroelastodynamics

- **Two compressional waves, one shear wave**
- **Waves are dispersive (wave speed is frequency dependent)**

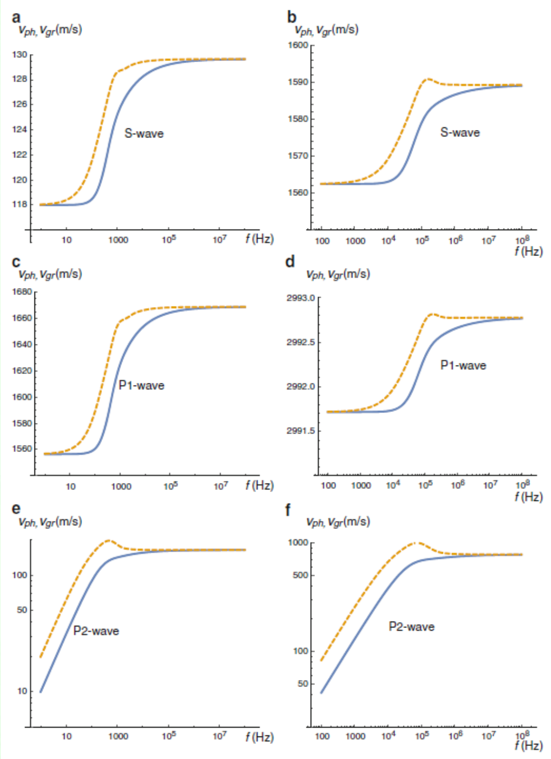

Fig. 9.5 Phase velocity (*solid line*) and group velocity (*dashed line*) as function of frequency for: shear wave (**a**) Hard sediment, (**b**) Berea sandstone; first compressional wave (**c**) Hard sediment, (**d**) Berea sandstone; and second compressional wave (**e**) Hard sediment, (**f**) Berea sandstone

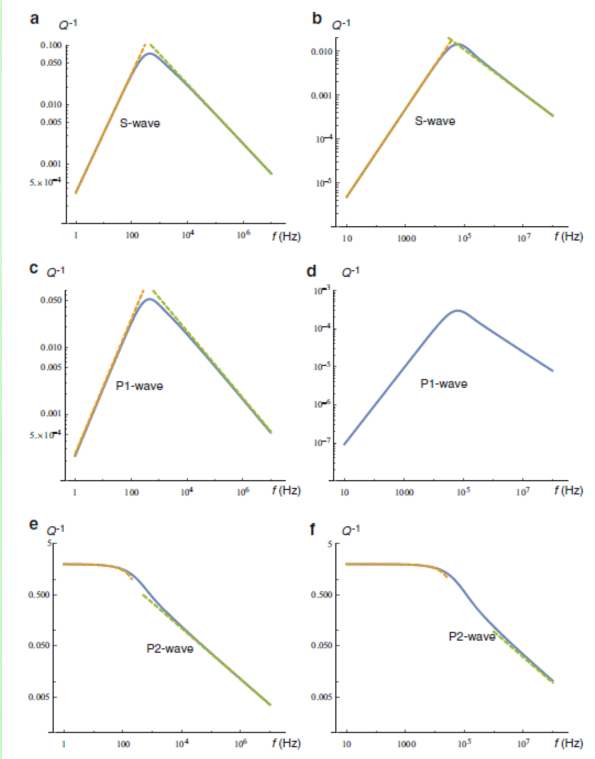

Fig. 9.6 Inverse quality factor (Q^{-1}) versus frequency for: shear wave (**a**) Hard sediment, (**b**) Berea sandstone; first compressional wave (**c**) Hard sediment, (**d**) Berea sandstone; and second compressional wave (**e**) Hard sediment, (**f**) Berea sandstone. *Dashed lines* are based on asymptotic formulae

Seismoelectric Exploration

- J-Effect: Change of electricity between two probes with the passage of elastic wave
- E-Effect: Naturally occurring electrical current ahead of earthquake wave.

Seismoelectromagnetic Effect

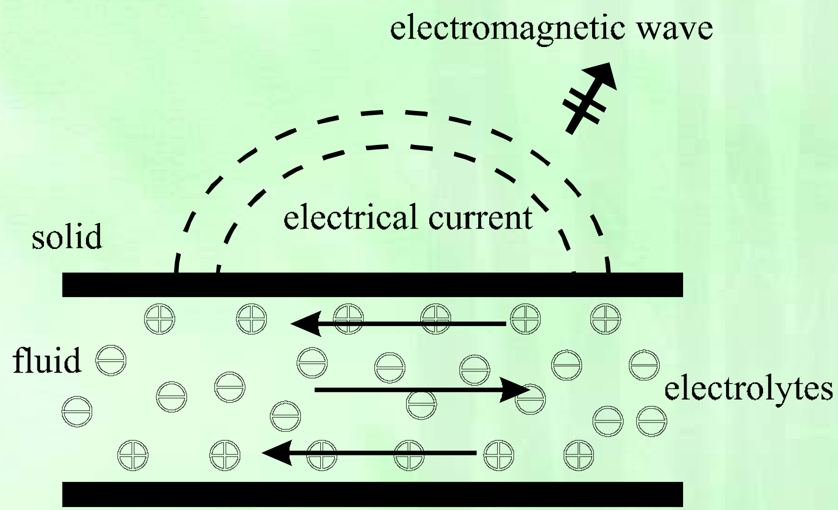

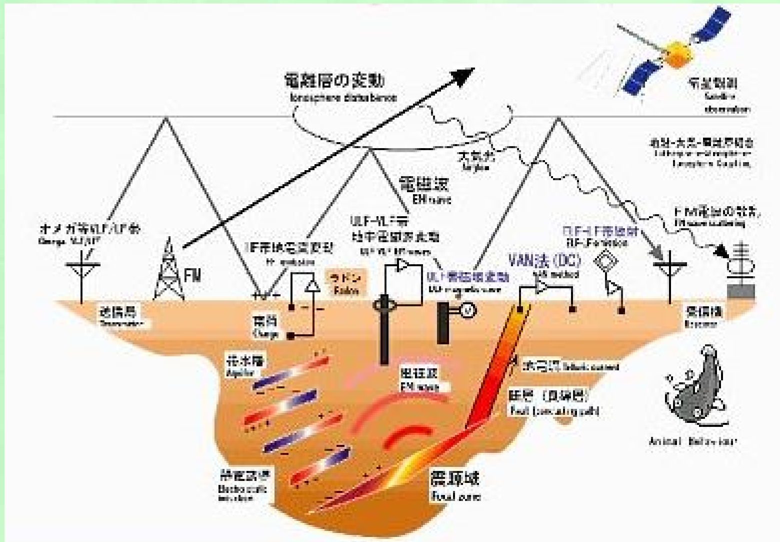

Typical Governing Equations: Poroelastodynamics

- Time domain

$$G\nabla^2\boldsymbol{u} + (\lambda_u + G)\nabla(\nabla\cdot\boldsymbol{u}) + \alpha M\nabla(\nabla\cdot\boldsymbol{w}) = \rho\ddot{\boldsymbol{u}} + \rho_f\ddot{\boldsymbol{w}} - \boldsymbol{F} + \alpha M\nabla Q$$

$$\alpha M\nabla(\nabla\cdot\boldsymbol{u}) + M\nabla(\nabla\cdot\boldsymbol{w}) - \frac{1}{\kappa}\dot{\boldsymbol{w}} = \rho_f\ddot{\boldsymbol{u}} + \rho'\ddot{\boldsymbol{w}} - \boldsymbol{f} + M\nabla Q$$

- Frequency domain

$$\begin{aligned} G\nabla^2\tilde{\boldsymbol{u}} + (\lambda_u + G)\nabla(\nabla\cdot\tilde{\boldsymbol{u}}) + \alpha M\nabla(\nabla\cdot\tilde{\boldsymbol{w}}) + \omega^2\rho\tilde{\boldsymbol{u}} + \omega^2\rho_f\tilde{\boldsymbol{w}} \\ = -\tilde{\boldsymbol{F}} + \alpha M\nabla\tilde{Q} \end{aligned}$$

$$\alpha M\nabla(\nabla\cdot\tilde{\boldsymbol{u}}) + M\nabla(\nabla\cdot\tilde{\boldsymbol{w}}) + \omega^2\rho_f\tilde{\boldsymbol{u}} + \omega^2\rho''\tilde{\boldsymbol{w}} = -\tilde{\boldsymbol{f}} + M\nabla\tilde{Q}$$

A.H.-D. Cheng,
Poroelasticity, Springer, 877 p., 2016.

Chapter 1 Introduction, 59 pages, free for download

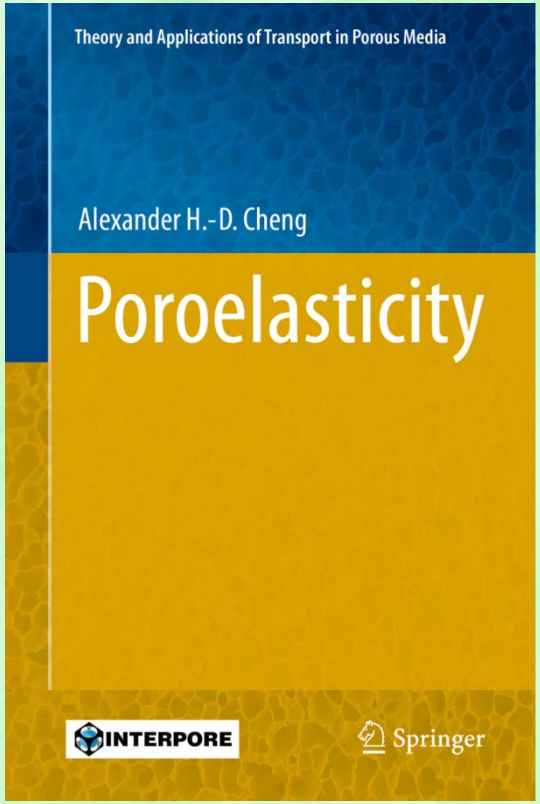

http://www.springer.com/us/book/9783319252001

THE END